Electronic structure and magnetic properties of $KCrSe_2$

1996 J. Phys.: Condens. Matter 8 4381

(http://iopscience.iop.org/0953-8984/8/24/007)

J. Phys.: Condens. Matter **8** (1996) 4381–4388. Printed in the UK

Electronic structure and magnetic properties of $KCrSe_2$

C M Fang, P R Tolsma, C F van Bruggen, R A de Groot, G A Wiegers and C Haas

Laboratory of Chemical Physics, Materials Science Centre of the University, Nijenborgh 4, 9747 AG Groningen, The Netherlands

Received 10 October 1995, in final form 27 February 1996

Abstract. $KCrSe_2$ characterized by x-ray powder diffraction is a layered compound isostructural with $NaCrSe_2$: $a = 3.80$ Å; $c = 22.19$ Å; space group $R\bar{3}m$. The magnetic properties are similar to those of $NaCrSe_2$ but with an even more pronounced difference between the intralayer and interlayer exchange interactions of Cr^{3+} $3d^3$ localized moments. The magnetic susceptibility above 100 K is of a Curie–Weiss nature; the Curie temperature is +250 K. An antiferromagnetic transition with $T_N = 40$ K occurs; in the ordered state, ferromagnetic layers are coupled antiferromagnetically. The analysis showed the intralayer exchange interaction J_1/k and interlayer exchange interaction J_2/k to be 16.7 K and −0.06 K, respectively.

A band-structure calculation using the LSW method was performed for $KCrSe_2$ in the ferromagnetic state (neglecting the interlayer antiferromagnetic ordering). The calculations show that $KCrSe_2$ is a semiconductor with a band gap of 0.7 eV. The potassium atoms are nearly ionized. The Cr $3d(t_{2g})$ states are completely spin polarized. The electronic configuration of Cr is $(3d)^3$, with a local magnetic moment of $3\mu_B$ per Cr atom.

1. Introduction

$NaCrS_2$, $NaCrSe_2$ and $KCrS_2$ have a simple layer structure based on cubic close packing of S^{2-} (Se^{2-}) anions. Na^+ (K^+) and Cr^{3+} ions occupy the octahedral holes between S^{2-} (Se^{2-}) layers in such a way that Na^+ (K^+) and Cr^{3+} layers alternate. Each Cr^{3+} ion has six in-plane nearest neighbours and $2 \times 3 = 6$ Cr^{3+} ions in the Cr^{3+} layers above and below the plane at much larger distance. These compounds show Curie–Weiss behaviour of the magnetic susceptibility with Curie temperature Θ of +30 K for $NaCrS_2$ [1, 2], +108 K for $NaCrSe_2$ [1, 2] and +112 K for $KCrS_2$ [3]. Antiferromagnetic ordering occurs in the temperature range 19–40 K. In the ordered state, as determined by neutron powder diffraction, ferromagnetic layers are coupled antiferromagnetically for $NaCrSe_2$ and $KCrS_2$, while for $NaCrS_2$ the ordering is helimagnetic in the layers and antiferromagnetic between layers [1–3]. The intralayer exchange interaction J_1 between nearest-neighbour Cr^{3+} ions consists of two contributions: a direct antiferromagnetic interaction J_1' and a ferromagnetic 90° superexchange interaction J_1''. The direct interaction J_1' depends strongly on the Cr–Cr distances; it is large for short Cr–Cr distances. The exchange interaction J_2 between Cr^{3+} ions of different layers is expected to be weak and antiferromagnetic. These rules explain in a natural way the change in Θ with a variation in the Cr–Cr distances. For compounds with relatively short Cr–Cr distances, Θ is negative (e.g., in $LiCrS_2$, the Cr–Cr distance is 3.464 Å and $\Theta = -276$ K [4]) while, for a compound with long Cr–Cr distances, Θ is positive (in $NaCrSe_2$, the Cr–Cr distance is 3.729 Å, $J_1/k = 8.9$ K and $J_2/k = -0.14$ K [1]; in $KCrS_2$, the Cr–Cr distance is 3.602 Å, $J_1/k = 7.6$ K and $J_2/k = -0.1$ K [3]).

0953-8984/96/244381+08$19.50

$KCrSe_2$ might be an interesting compound since the difference between interlayer and intralayer exchange is expected to be even more pronounced than for $NaCrSe_2$, because of the expected larger distance between the Cr^{3+} ions. In this paper the structure and magnetic properties of $KCrSe_2$ are reported. Some of the results have already been reported in conference proceedings [5]. A band-structure calculation of $KCrS_2$ was published; however, the unit-cell dimensions used were those of $KCrS_2$ [6]. A new band-structure calculation based on the correct structure was carried out and will be discussed.

2. Experimental details

$KCrSe_2$ was prepared by direct combination of the elements in evacuated quartz tubes, first slowly heated to about 200 °C during which the reaction of potassium with selenium takes place, then kept at 800 °C for 5 days, followed by slow cooling to room temperature. The powder samples were characterized by x-ray powder diffraction. $KCrSe_2$ obtained by slow cooling is isostructural with $NaCrS_2$, $KCrS_2$ and $NaCrSe_2$. The unit-cell dimensions are $a = 3.801(1)$ Å, $c = 22.19(1)$ Å (average for three samples); the space group is $R\bar{3}m$ and $Z = 3$. The atoms are at the following Wyckoff positions: 3(a), (0,0,0) (Cr); 3(b), $(0,0,\frac{1}{2})$ (K); 6(c), $\pm(0, 0, z)$ (Se) with $z = 0.275$ (z was obtained from a comparison of observed and calculated intensities). It may be noted that by quenching from a high temperature, orthorhombic structures were found, identical with those of $K_{0.9}CrSe_2$ samples [7].

Magnetic properties in the temperature range 4–300 K were measured using an Oxford Instruments Faraday balance equipped with superconducting coils. In the temperature range 100–1000 K an Oxford Instruments high-temperature Faraday balance was used.

3. Magnetic properties

The reciprocal magnetic susceptibility versus temperature curve of $KCrSe_2$ powder measured at a field of 8.61 kOe is shown in figure 1. The behaviour is of Curie-Weiss type in the range 500–1000 K. The Curie constant C_m obtained from a fit in this temperature range is 1.88 cm^3 K mol^{-1}, in good agreement with the Curie constant of 1.875 for Cr^{3+} $3d^3$, $S = \frac{3}{2}$. The asymptotic Curie temperature Θ is +250 K. In the temperature range 125–500 K the increase in χ^{-1} is due to short-range order, making $\Theta > T_N$. In the low-temperature range (inset of figure 1) the inverse susceptibility shows the typical behaviour of antiferromagnetic ordering: $T_N = 40$ K. The field dependence of the magnetization at 5.5 K is shown in figure 2. The curve shows a small change in slope at about 5 kOe and saturation at 13 kOe at $M_{tot} = 14.5 \times 10^{-3}$ G cm^3 mol^{-1}, corresponding to a magnetic moment of $2.6\mu_B$ per Cr atom. At this field the magnetic moments are all parallel.

The sum of the intralayer exchange J_1 and the interlayer exchange J_2 can be obtained from Θ using molecular-field theory

$$k\Theta = \tfrac{2}{3}S(S+1)(6J_1 + 6J_2). \tag{1}$$

One finds that $(J_1 + J_2)/k = 16.7$ K. A better way is to go beyond molecular-field theory by using a series expansion of χ^{-1} [8, 9]. For the Heisenberg triangular lattice with $S = \frac{3}{2}$ in the temperature range 50–500 K this reads

$$\chi^{-1} = 3J/Ng^2\mu_B^2[x + 4 + 3.20/x - 2.816/x^2 + 0.08/x^3 + 3.45/x^4 - 3.99/x^5 + \cdots] \tag{2}$$

with $x = kT/J_1$. In this way, one obtains $J_1/k = 16.0(2)$ K.

The value of J_2 can be obtained from the relation for mean-field theory:

$$\chi^{-1}(T_N)C_M = 8J_2S(S+1)/k. \tag{3}$$

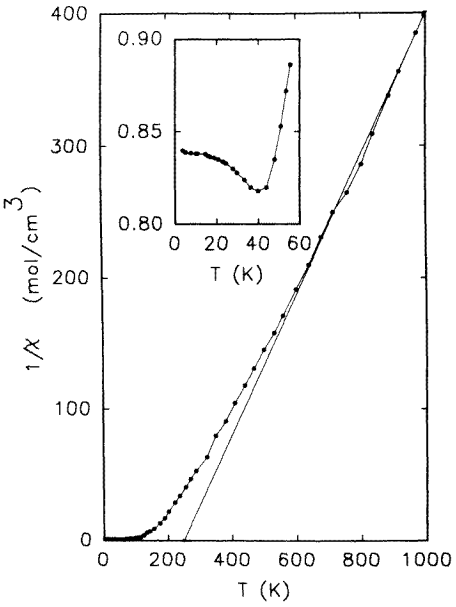

Figure 1. Reciprocal magnetic susceptibility χ^{-1} versus temperature measured at 8.6 kOe. The inset shows χ^{-1} in the low-temperature region.

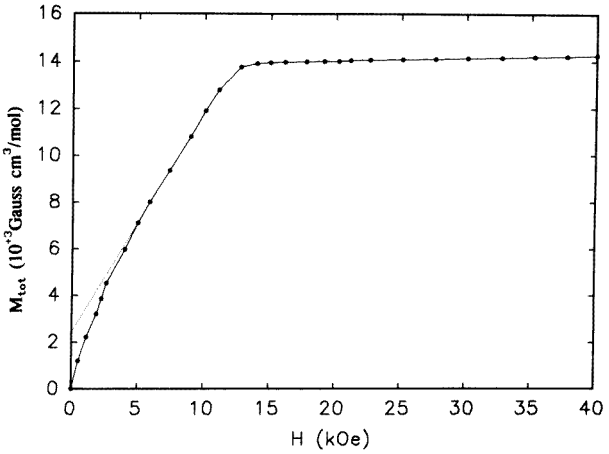

Figure 2. Magnetization versus magnetic field at 5.5 K.

For $KCrSe_2$, one finds in this way that $J_2/k = -0.05$ K.

An accurate value of J_2 can be obtained from the magnetization versus field curve. At low temperatures the sublattice magnetizations M_1 and M_2 of alternating layers of Cr^{3+} ions are nearly saturated: $M_1 = M_2 = \frac{1}{2}Ng\mu_B S$, where N is the number of Cr^{3+} ions and $g = 2$, $S = \frac{3}{2}$. Applying a magnetic field $\boldsymbol{H}$ will result in orienting the sublattice magnetizations $\boldsymbol{M}_1$ and $\boldsymbol{M}_2$ along $\boldsymbol{H}$. For Cr^{3+} ions, one expects that the magnetic anisotropy is very

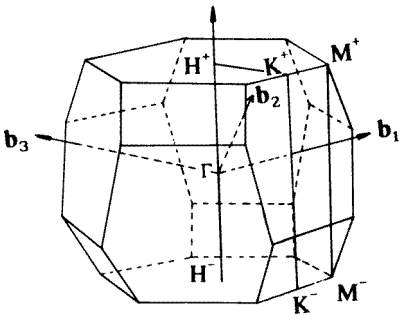

Figure 3. Brillouin zone and high-symmetry points of $KCrSe_2$.

small. In that case the energy U is given by

$$U = -\tfrac{1}{2}\alpha(\boldsymbol{M}_1^2 + \boldsymbol{M}_2^2) - \alpha'\boldsymbol{M}_1 \cdot \boldsymbol{M}_2 - (\boldsymbol{M}_1 + \boldsymbol{M}_2) \cdot \boldsymbol{H}$$
$$= -\alpha M^2 - \alpha' M^2 \cos(180 - 2\phi) - 2MH \sin\phi \qquad (4)$$

with $M = |\boldsymbol{M}_1| = |\boldsymbol{M}_2|$; $\alpha = 4zJ_1/Ng^2\mu_B^2$, $\alpha' = 4zJ_2/Ng^2\mu_B^2$; $z = 6$ is the number of nearest neighbours. The angle between the field $\boldsymbol{H}$ and $\boldsymbol{M}_1$ and $\boldsymbol{M}_2$ is $90 - \phi$.

From the condition $\delta U/\delta\phi = 0$, one finds that $\sin\phi = -H/2\alpha' M$. The magnetization for a field $H < H_0$ is given by $M_{tot} = 2M\sin\phi = -H/\alpha'$. For a magnetic field $H > H_0$, the sublattice magnetizations are parallel to the field ($\phi = 90^\circ$; $M_{tot} = 2M_0$). The saturation field H_0 is given by $H_0 = -2\alpha' M$. From this, one calculates, with $H_0 = 13$ kOe and $M_{tot} = 14.5 \times 10^3$ G cm^3 mol^{-1}, that $J_2/k = -0.058$ K, in good agreement with the value -0.05 K from mean-field theory.

The energy difference between the ferromagnetic state and the antiferromagnetic state (for $H = 0$) can also be obtained from the M versus H curve: $E_F - E_{AF} = H_0 M = 1 \times 10^{-4}$ eV per Cr (for a magnetic moment of $2.6\mu_B$/Cr for H_0 at 5.5 K).

4. Band-structure calculation

Ab-initio band-structure calculations were performed with localized spherical wave (LSW) [10] method using a scalar-relativistic Hamiltonian. We used local-density exchange–correlation potentials [11] inside space filling, and therefore overlapping Wigner–Seitz spheres around the atomic constituents. The self-consistent calculations were carried out including all core electrons.

Iterations were performed with 344 $\boldsymbol{k}$-points distributed uniformly in the irreducible part of the first Brillouin zone (BZ). Self-consistency was assumed when the changes in the local partial charges in each atomic sphere decreased to the order of 10^{-5}.

In the construction of the LSW basis [10, 12], the spherical waves were augmented by solution of the scalar-relativistic radial equations, characterized by atomic-like 4s, 4p and 3d orbitals corresponding to the valence levels of the parent elements K, Cr and Se. The internal l summation used to augment the Hankel function at surrounding atoms, was extended to $l = 3$, resulting in the use of 4f orbitals for Cr and Se. When the crystal is not very densely packed, it is necessary to include empty spheres in the calculation. In our case, empty spheres located at $(\frac{1}{2}, \frac{1}{2}, \frac{1}{2})$ were sufficient. The functions 1s, 2p and 3d were used for the empty spheres. The calculations which were performed for ferromagnetic and

Table 1. Input parameters of atoms (Cr, K and Se) and empty spheres (Va) for the band-structure calculation of ferromagnetic $KCrSe_2$. R_{WS} represents the Wigner–Seitz radius (space group, $R\bar{3}m$ (No. 166); $a = 3.80$ Å; $c = 22.19$ Å).

Atom		x	y	z	R_{WS} (Å)	Starting configuration
Cr	3a	0	0	0	1.1632	$[Ar]4s^{0.5}4p^{0.0}3d^{3.0}4f^{0.0}$ (spin up)
						$[Ar]4s^{0.5}4p^{0.0}3d^{2.0}4f^{0.0}$ (spin down)
K	3b	0	0	$\frac{1}{2}$	1.1632	$[Ar]4s^{0.5}4p^{0.0}3d^{0.0}$ (spin up and down)
Se	6c	0	0	0.275	1.9193	$[Ar]4s^{1.0}4p^{2.0}4d^{0.0}4f^{0.0}$ (spin up and down)
Va	9d	$\frac{1}{2}$	$\frac{1}{2}$	$\frac{1}{2}$	1.1632	$1s^{0.0}2p^{0.0}3d^{0.0}$ (spin up and down)

Table 2. Charge Q and atomic configuration of atoms (K, Cr and Se) and empty spheres (Va) for ferromagnetic $KCrSe_2$.

Atom	Q	Electronic configuration
Cr	+1.88	$[Ar]4s^{0.08}4p^{0.10}3d^{3.33}4f^{0.01}$ (spin up)
		$[Ar]4s^{0.07}4p^{0.08}3d^{0.43}4f^{0.01}$ (spin down)
K	+0.97	$[Ar]4s^{0.01}4p^{0.01}3d^{0.00}$ (spin up)
		$[Ar]4s^{0.01}4p^{0.01}3d^{0.00}$ (spin down)
Se	−1.27	$[Ar]4s^{0.97}4p^{2.34}3d^{0.22}4f^{0.11}$ (spin up)
		$[Ar]4s^{0.98}4p^{2.50}3d^{0.11}4f^{0.04}$ (spin down)
Va	−0.10	$1s^{0.02}2p^{0.02}3d^{0.01}$ (spin up and down)

Table 3. Energies (with respect to the top of the valence band) and symmetry (labels according to Miller and Love [13]) at Γ for $KCrSe_2$; OC represents the dominant orbital character.

Spin up			Spin down		
Energy (eV)	Symmetry	OC	Energy (eV)	Symmetry	OC
−13.73	1^+	Se(4s)	−13.73	1^+	Se(4s)
−12.45	2^-	Se(4s)	−12.52	2^-	Se(4s)
−4.67	1^+	Se($4p_z$)	−4.39	1^+	Se($4p_z$)
−3.17	3^+	Se($4p_x$,$4p_y$)	−2.25	3^+	Se($4p_x$,$4p_y$)
−1.20	3^+	Cr($3d_{xy}$,$3d_{xz}$,$3d_{yz}$,$3d_{xx}$)	−0.87	2^-	Se($4p_z$)
−0.84	2^-	Se($4p_z$)	−0.31	3^-	Se($4p_x$,$4p_y$)
−0.45	1^+	Cr($3d_{zz}$)	+1.24	3^+	Cr($3d_{xy}$,$3d_{xz}$,$3d_{yz}$,$3d_{xx}$)
−0.28	3^-	Se($4p_x$,$4p_y$)	+1.85	1^+	Cr($3d_{zz}$)
+1.79	3^+	Cr($3d_{xy}$,$3d_{xz}$,$3d_{yz}$,$3d_{xx}$)	+3.48	3^+	Cr($3d_{xy}$,$3d_{xz}$,$3d_{yz}$,$3d_{xx}$)

antiferromagnetic $KCrSe_2$ show that the energy difference between the ferromagnetic and antiferromagnetic state is very small (about 0.001 eV, in the error range of calculations) and their electronic structures are nearly the same except for the different magnetic orderings. This is in agreement with the magnetic measurements. Here we report only the results of calculations for ferromagnetic $KCrSe_2$. The input parameters (space group, unit cell, atomic positions, Wigner–Seitz radii and starting electronic configurations) are listed in table 1.

The results of the calculation (electronic configuration and charges) are shown in table 2. Table 3 lists the energy, symmetry and orbital characters of the energy bands at Γ for $KCrSe_2$. The Brillouin zone is depicted in figure 3. The density of states of ferrromagnetic $KCrSe_2$ is shown in figure 4. The energy bands along high-symmetry directions in the hexagonal Brillouin zone are shown in figure 5 for spin up and figure 6 for spin down.

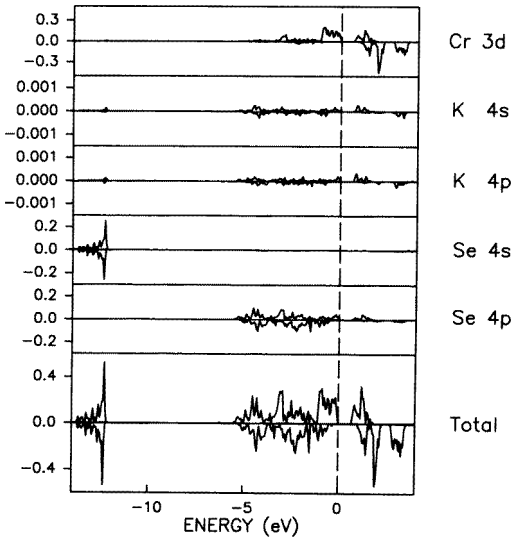

Figure 4. Partial and total densities of states of $KCrSe_2$. The positive and negative parts represent the densities of state for spin-up and spin-down electrons, respectively.

The calculated band structure shows that the occupations of the K 4s and K 4p states are very small (table 2 and figure 4). Then each K atom has donated one electron to the $CrSe_2$ part.

The lowest two energy bands ranging from -13.8 to -12.2 eV consist mainly of Se 4s orbitals; these bands are well separated from the other bands by an energy gap of about 6.7 eV.

The valence bands range from -5.5 to 0.0 eV (energies with respect to the top of the valence bands) for the spin-up electrons, and from -5.3 to -0.3 eV for the spin-down electrons.

The dispersion curves, given in figures 5 and 6, show that the band dispersion in directions parallel to $\boldsymbol{k}_z$ (H^+–H^-, M^+–M^- and K^+–K^-) is small (about 0.5 eV) compared with that in the directions perpendicular to $\boldsymbol{k}_z$ (about 2–3 eV). The small dispersion along $\boldsymbol{k}_z$ is due to the large distances between the $CrSe_2$ sandwiches which are separated by the K atoms, and by the absence of K states in this energy range. These effects prevent appreciable covalent interlayer interactions between the $CrSe_2$ sandwiches. A direct consequence is that interlayer superexchange interactions are expected to be quite small, as is demonstrated indeed by the small value of J_2 in $KCrSe_2$. It also follows that the interlayer bonding is mainly due to ionic interactions between K^+ ions and the negatively charged $CrSe_2^-$ sandwiches.

The Cr 3d states are nearly completely spin polarized, i.e. only Cr 3d orbitals for spin-up electrons are occupied. The local moments on Cr are about $3\mu_B$. The Cr 3d bands in $KCrSe_2$ are rather narrow, in contrast with the much wider Cr 3d bands in CrSe [14] and 1T-$CrSe_2$ [15]. The Cr 3d bands show an exchange splitting ΔE_{ex} of about 3.0 eV between the states for spin-up and spin-down electrons. For CrSe the exchange splitting is $\Delta E_{ex} = 2.7$ eV [14]. The exchange splitting is expected to be proportional to the quantum number S. For CrSe, $S = 2$ and, for $KCrSe_2$, $S = \frac{3}{2}$, so that we expect $\Delta E_{ex}(KCrSe_2)/\Delta E_{ex}(CrSe) = \frac{3}{2}/2 = \frac{3}{4}$. This is close to the value deduced from band-structure calculations, which is $2.0/2.7 = 0.74$.

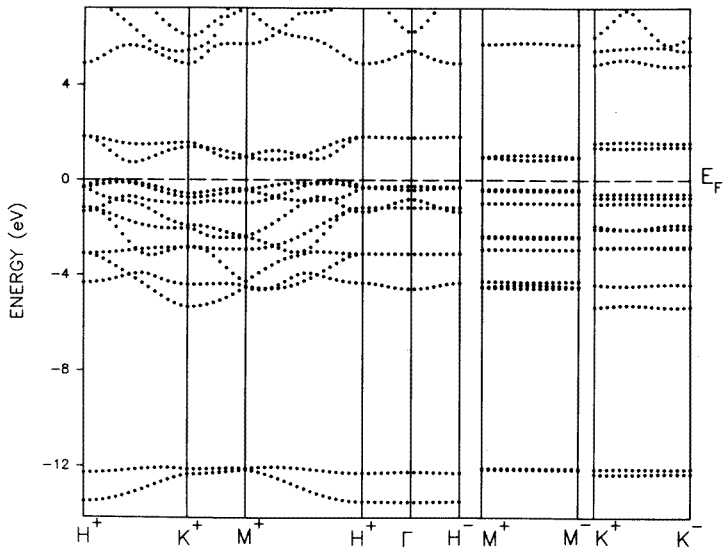

Figure 5. Dispersion of the energy bands for spin-up electrons for $KCrSe_2$.

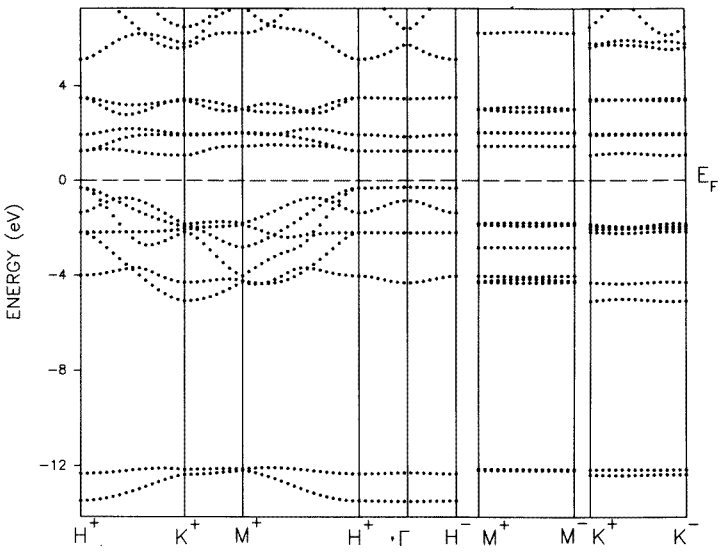

Figure 6. Dispersion of the energy bands for spin-down electrons for $KCrSe_2$.

The t_{2g}–e_g splitting of the Cr 3d bands in a trigonally distorted octahedral ligand field is clearly observed. This crystal field splitting $E(e_g) - E(t_{2g})$ is about 1.6 eV (1.7 eV for spin-up and 1.5 eV for spin-down states).

According to the band-structure calculations, $KCrSe_2$ is a semiconductor with an energy gap of about 0.7 eV. The top of the valence band and the bottom of the conduction band are both Cr 3d spin-up states, strongly hybridized with Se 4p states. Thus $KCrSe_2$ is a

Mott–Hubbard insulator in the classification by Zaanen *et al* [16].

Band-structure calculations were performed for the isostructural compound $NaCrS_2$ by Sebilleau *et al* [17] using the LMTO ASA method. The electronic structure of $KCrSe_2$ is similar to that of $NaCrS_2$, but there are some differences. The difference between the total energies of antiferromagnetic and ferromagnetic ordering is 0.006 eV in $NaCrS_2$, which is much larger than that of $KCrSe_2$ (about 0.001 eV). That is due to the much larger $|J_2/k|$ for $NaCrS_2$ ($J_2/k = -0.8$ K) than for $KCrSe_2$ ($J_2/k = -0.05$ K). Here we compare our results with the calculations for ferromagnetic $NaCrS_2$. It is remarkable that the Cr 4s states in $KCrSe_2$ are well separated from the Cr 3d bands (the energy gap is about 4.0 eV for spin-up and 2.0 eV for spin-down electrons), which is different from those of $NaCrS_2$ (about 0.33 eV for spin-up and overlap for spin-down electrons). The t_{2g} band width is larger in $KCrSe_2$ (1.1 eV for spin-up and 1.3 eV for spin-down electrons) than in $NaCrS_2$ (0.72 and 0.94, respectively), and the $t_{2g} - e_g$ band gaps are different for $KCrSe_2$ (0.69 eV for spin-up and 0.50 eV for spin-down electrons) compared with those of $NaCrS_2$ (1.16 eV and -0.12 eV for spin-up and spin-down electrons, respectively). These effects are due to the more covalent nature of the bonding in $KCrSe_2$.

5. Conclusions

$KCrSe_2$ is antiferromagnetic with a Curie temperature $\Theta = +250$ K and an ordering temperature $T_N = 40$ K. The magnetic structure consists of ferromagnetic layers coupled antiferromagnetically. The magnetic properties of $KCrSe_2$ are similar to those of $NaCrSe_2$ and $KCrS_2$, but with an even larger ratio $|J_1/J_2|$. J_1 for $KCrSe_2$ is larger than J_1 for $NaCrSe_2$ because of the larger intralayer Cr–Cr distances in $KCrSe_2$.

The calculated band structure of $KCrSe_2$ indicates that $KCrSe_2$ is a semiconductor with an energy gap of 0.7 eV. The top of the valence band and the bottom of the conduction band both have Cr 3d spin-up character, so that $KCrSe_2$ is a Mott–Hubbard semiconductor. The Cr 3d states are completely spin polarized, resulting an electronic configuration Cr $(3d)^3$ and a magnetic moment $3\mu_B$ per Cr atom.

References

[1] Bongers P F, van Bruggen C F, Koopstra J, Omloo W P F A M, Wiegers G A and Jellinek F 1968 *J. Phys. Chem. Solids* **29** 977
[2] Engelsman F M R, Wiegers G A, Jellinek F and van Laar B 1973 *J. Solid State Chem.* **6** 574
[3] van Laar B and Engelsman F M R 1973 *J. Solid State Chem.* **6** 384
[4] van Laar B and Ydo D J W 1971 *J. Solid State Chem.* **3** 590
[5] *Collected Abstracts, 7th Int. Conf. on Solid Compounds of Transition Elements (Stuttgart, 1979)*
[6] Dijkstra K, van Bruggen C F, Haas C and de Groot R A 1989 *Phys. Rev.* B **40** 7973
[7] Tolsma P 1973 *Laboratory of Inorganic Chemistry, University of Groningen, Internal Report*
[8] Cross C, Niel M, LeFlem G, Pouchard M and Hagenmuller P 1975 *Mater. Res. Bull.* **10** 461
[9] Rushbrooke G S and Wood P J 1963 *Mol. Phys.* **6** 409
[10] van Leuken H, Lodder A, Czyzyk M T, Springelkamp F and de Groot R A 1990 *Phys. Rev.* B **41** 5613
[11] Hedin L and Lundqvist B I 1971 *J. Phys. C: Solid State Phys.* **4** 2064
[12] Methfessel M and Kubler J 1982 *J. Phys. F: Met. Phys.* **12** 141
[13] Miller S C and Love W F 1967 *Tables of Irreducible Representations of Space Groups and Representations of Magnetic Space Groups* (Boulder, CO: Pretty Press)
[14] Dijkstra J, van Bruggen C F, Haas C and de Groot R A 1989 *J. Phys.: Condens. Matter* **1** 9163
[15] Fang C M, Haas C, Wiegers G A and de Groot R A 1996 to be published
[16] Zaanen J, Sawatzky G A and Allen J W 1985 *Phys. Rev. Lett.* **55** 418
[17] Sebilleau D, Guo G Y and Temmerman W M 1989 *J. Phys.: Condens. Matter* **1** 5653